Recent results on electron cyclotron current drive and MHD activity in RTP

RECENT RESULTS ON ELECTRON CYCLOTRON CURRENT DRIVE AND MHD ACTIVITY IN RTP

A.J.H. DONNÉ, F.C. SCHÜLLER, A.A.M. OOMENS,
M. DE BAAR, C.J. BARTH, M.N.A. BEURSKENS, F.M.A. BOX,
J.F.M. VAN GELDER, B.J.J. GROBBEN, B. DE GROOT,
J.M. HERRANZ, G.M.D. HOGEWEIJ, S.A. HOKIN[1],
J. HOWARD[2], C.A.J. HUGENHOLTZ, F.A. KARELSE,
J. DE KLOE, O.G. KRUIJT, S. KUYVENHOVEN, J. LOK,
N.J. LOPES CARDOZO, H.J. VAN DER MEIDEN, F.G. MEIJER,
A. MONTVAI, T. OYEVAAR, F.J. PIJPER, R.W. POLMAN,
J.H. ROMMERS, F. SALZEDAS, B.C. SCHOKKER, P.H.M. SMEETS,
C.P. TANZI, C.J. TITO, G.C.H.M. VERHAAG, E. WESTERHOF
FOM Instituut voor Plasmafysica 'Rijnhuizen',
Association Euratom–FOM,
Nieuwegein, Netherlands

Abstract

RECENT RESULTS ON ELECTRON CYCLOTRON CURRENT DRIVE AND MHD ACTIVITY IN RTP.

The RTP tokamak ($R = 0.72$ m, $a = 0.164$ m, $B_\phi < 2.5$ T, $I_p = < 150$ kA) is equipped with three gyrotrons (2 × 60 GHz, 180 kW, 100 ms each; 1 × 110 GHz, 500 kW, 200 ms) for electron cyclotron heating (ECH) and current drive (ECCD). The power from one of the 60 GHz gyrotrons is launched via an adjustable mirror from the high field side (HFS) in the 1X-mode. The power of both other gyrotrons is sent in perpendicularly to the toroidal magnetic field from the low field side (LFS). A comprehensive set of high-resolution multichannel plasma diagnostics is available to study the detailed behaviour of various plasma phenomena. First, recent diagnostic innovations are briefly discussed. Then, new physics results are presented for ohmic and EC heated plasmas. ECCD, slide-away discharges, discharges with a hollow temperature profile and MHD phenomena, including sawteeth and disruptions, are treated.

1. DIAGNOSTIC INNOVATIONS

The 20-channel heterodyne radiometer for studying electron cyclotron emission (ECE) in the 2nd harmonic X-mode has been extended with an antenna at the HFS, that is connected to a sweep-tuneable microwave source [1]. In this way the electron pressure profile, $p_e(r)$, can be deduced from the optical thickness profile, $\tau(r)$, measured by means of electron cyclotron absorption (ECA). By sweeping the source, ECE and ECA measurements are performed alternatingly during the discharge. After accounting for non-resonant effects (e.g. refraction,

[1] Royal Institute of Technology, Stockholm, Sweden.
[2] Australian National University, Canberra, Australia.

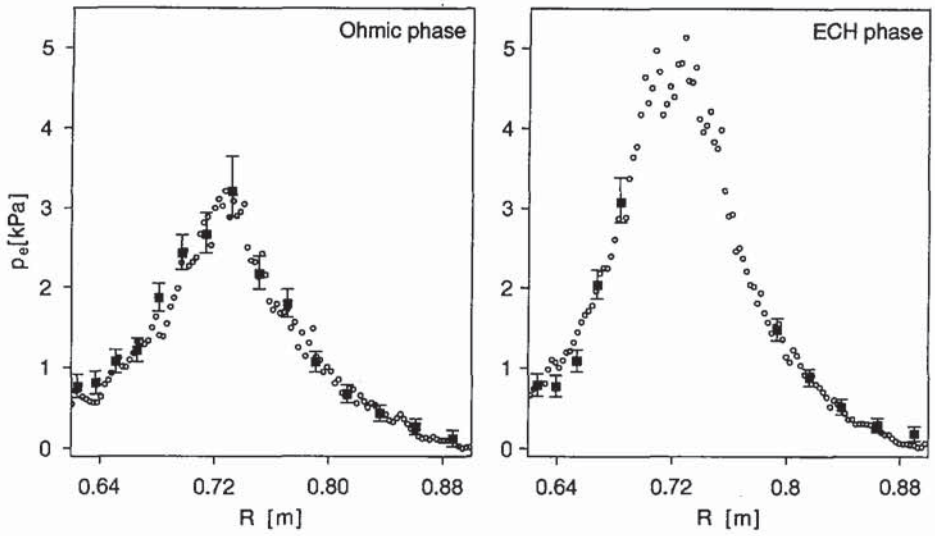

Fig. 1. Pressure profiles measured by ECA (full squares) and Thomson scattering (open circles) during the ohmic and the ECH phase of a discharge. During the ECH phase no information can be obtained with the central five channels since the plasma is optically thick for the corresponding frequencies.

scattering, mode conversion) a very good agreement is found between the p_e profiles measured with ECA and those obtained from Thomson scattering (see Fig. 1). Since the RTP plasmas are semi-opaque under most experimental conditions, the measured values for τ can be used to correct the $T_e(r)$ for finite optical thickness effects. Finally, by combining $p_e(r)$ determined from ECA with $n_e(r)$ from the 19-channel interferometer an electron temperature profile can be derived that is insensitive to non-thermal electron populations.

The HFS horn allowed comparison between ECE received at the HFS and the LFS. The difference between the two spectra is directly related to the existence of a suprathermal electron population. Simulation with Fokker-Planck codes including particle diffusivity and EC emissivity showed excellent agreement with the experimental LFS/HFS spectra.

The far-infrared interferometer was recently extended with a polarimeter option [2]: the Faraday rotation is measured along 19 vertical chords. Three CO_2-pumped far-infrared lasers are employed to simultaneously measure the refractive indices for the two polarisation eigenstates in the plasma. The time resolution of the device is determined by the signal-to-noise ratio only and can be as high as 100 kHz. A resolution of 10 kHz and an accuracy of better than 0.2° have already been obtained. The interferometer/polarimeter has been successfully used to study the dynamic behaviour of the electron density and current density profiles at higher densities, as a response to externally induced perturbations like ECH and pellet injection. Unfortunately, at the low density needed for significant ECCD the error bars became too large to extract reliable information on the distribution of the driven current.

2. ELECTRON CYCLOTRON CURRENT DRIVE (ECCD)

ECCD is accomplished by preferentially heating electrons moving in one toroidal direction. Their reduced collisionality results in a toroidal current. In RTP ECCD has been achieved in the down-shifted resonance scheme. The dependence of I_{ECCD} on the location of the resonance layer and on the toroidal launch angle has been measured. The results are compared with Fokker-Planck simulations which take into account radial transport of non-thermal electrons, and which have been carried out for the parameters covered by the experiments.

The linearly polarised waves are obliquely launched from the HFS via a flat adjustable mirror, located halfway the equatorial plane and the top. The launch angles range from -30° to +30° off-perpendicular (standard settings) in the toroidal direction. In the poloidal plane the power is directed downwards towards the magnetic axis. Most experiments have been done with a power of about 130 kW and pulse lengths of up to 100 ms, I_p = 60 kA, $T_e(0) \approx 1.5$ keV, and $\langle n_e \rangle \approx (1.0 - 1.3)\times 10^{19}$ m^{-3}; B_ϕ was varied between 2.1 and 2.5 T. In some discharges a second gyrotron was used to achieve higher temperatures of the target plasma ($T_e(0) \approx 3$ keV). The density was feedback controlled.

In RTP — apart from a few experiments with constant inductively coupled power [3]— the total plasma current, I_p, is kept constant by a feedback circuit. The established ECCD is not large enough to drive I_p completely, and so the loop voltage is only reduced below its ohmic value. The EC driven currents have been derived from a comparison of the residual loop voltages for co- and counter-drive discharges: $I_{ECCD} = [(V_{cntr} - V_{co}) / (V_{cntr} + V_{co})] (I_p - I_{boot})$, where V_{cntr} and V_{co} represent the loop voltages during counter- and co-drive, respectively; the bootstrap current, I_{boot}, is small and has been taken zero. The experimental results are summarised in Fig. 2.

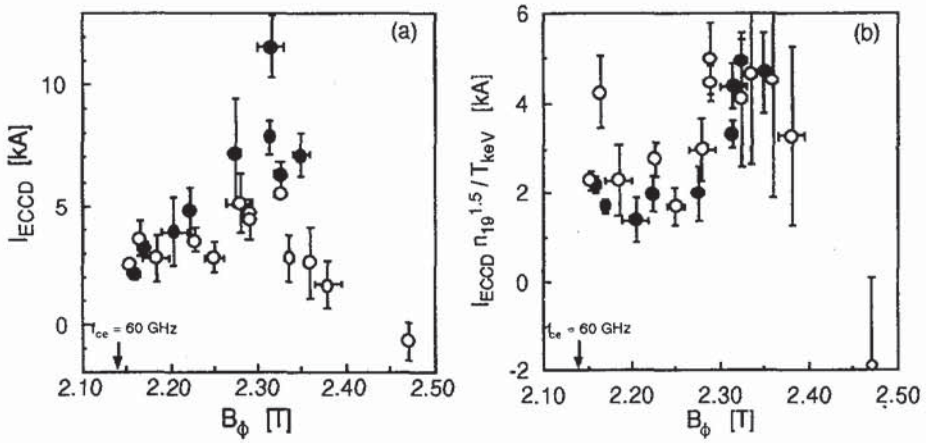

Fig. 2. Experimental I_{ECCD} as a function of B_ϕ for 30° off-perpendicular injection. Open and full circles: One and two gyrotrons respectively; (a) I_{ECCD}; (b) I_{ECCD} normalised with a scaling factor $n^{1.5}/T$.

Linear theory predicts for the scaling with temperature and density $I_{ECCD} \sim T_e/n_e$; the Fokker-Planck simulations suggest for the RTP regime an even stronger influence of the density: $I_{ECCD} \sim T_e/n_e^{1.5}$, where the temperature scaling may be complicated further by a dependence on the magnetic field on axis. The temperature effect is clearly demonstrated in Fig. 2a. The maximum driven current (11 kA) was obtained at $B_\phi = 2.33$ T for $T_e \approx 3$ keV and $\langle n_e \rangle \approx 1.0 \times 10^{19}$ m^{-3}. This is consistent with the largest possible resonance downshift at the plasma centre while still retaining efficient central heating. For one gyrotron the maximum temperature reached is lower ($T_e \approx 1.5$ keV) and the I_{ECCD} shows a maximum (≈ 6 kA) at $B_\phi \approx 2.30$ T. For higher values of the magnetic field (2.46 T) the off-axis heating leads to a decreased central temperature during ECH — this resembles 2X-mode off-axis heating results with the 110 GHz gyrotron [4] — and, apparently, to a small negative current. The dependence on B_ϕ is in qualitative agreement with predictions (see Fig. 3a).

Current drive results at the non-standard injection angles ±23° and ±11° indicate a decrease in efficiency as theory predicts, but error bars are too large for a quantitative comparison with the numerical predictions given in Fig. 3a. Results at the different plasma currents of 40 and 80 kA are, so far, not distinguishable from 60 kA results.

Fokker-Planck calculations, without inclusion of radial transport, predict the local generation of high-energetic electron populations. In many cases, these non-thermal electrons may locally even account for an equal or even much higher energy density than the thermal plasma. This is shown in Fig. 3b for a case with both LFS O-mode heating and HFS X-mode ECCD. The large population of energetic electrons is reflected by a strong increase of $T_e = (2/3\ \varepsilon/n_e)$, where ε is the energy density. When radial transport is included in the calculations with a relatively large anomalous diffusion coefficient $D = (1 + 3\ (r/a)^2)$ m^{2}s^{-1}, the

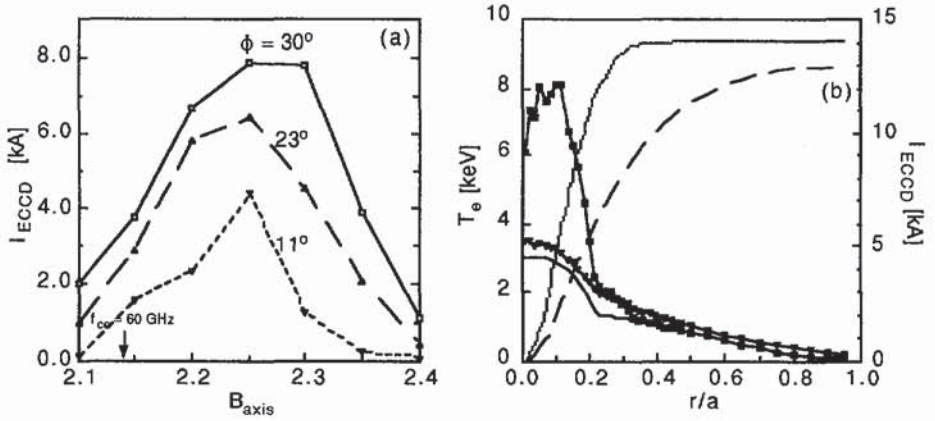

Fig. 3. (a) Simulated I_{ECCD} as function of B_ϕ for 11°, 23°, and 30° off-perpendicular injection. Plasma parameters: $T_e(0) = 1.5$ keV, $n_e(0) = 1.7 \times 10^{19}$ m^{-3}, EC power: 135 kW X-mode. (b) Simulated profiles of "temperature" (i.e. 2/3 of energy density divided by the particle density) and integrated EC driven current profile without (squares, dotted curve) and with (triangles, long-dashed curve) the inclusion of anomalous radial diffusion. The same density and ECH X-mode power were used as in (a), but additionally 120 kW of ECH O-mode power (LFS) was included. The full curve without symbols gives the input T_e-profile.

highly localised non-thermal electrons are redistributed such that globally the contribution of non-thermal electrons is almost the same and the total EC driven current decreases only slightly (by at most 20%). In these calculations the anomalous inward pinch was chosen such that the density profile was not affected. As mentioned in Sect. 1 these types of Fokker-Planck calculation lead also to accurate predictions of ECE-spectra measured both from LFS and HFS side.

3. SLIDE-AWAY DISCHARGES

A comprehensive study of slide-away (SA) discharges was carried out [5], with emphasis on the diagnosis of the non-thermal electron population using ECE (both X and O-mode, and including HFS measurements). Also the influence of ECH on a slide-away discharge was investigated (see Fig. 4). It was shown that at $n_e(0) < n_{c1} = 1 \times 10^{19}$ m^{-3} the discharge is always in SA, whereas it never is at $n_e(0) > n_{c2} = 2 \times 10^{19}$ m^{-3}. At the intermediate densities, application of a short ECH pulse always brings the discharge in SA. The intensity of the emission at the Lower Hybrid frequency was measured and shown to be linearly proportional to the run-away birth rate over four orders of magnitude. The high intensity of the measured ECE spectra requires a large ($\approx$ 5%) population of trapped electrons, with energies up to 30 keV, as compared to 1 keV for the bulk plasma.

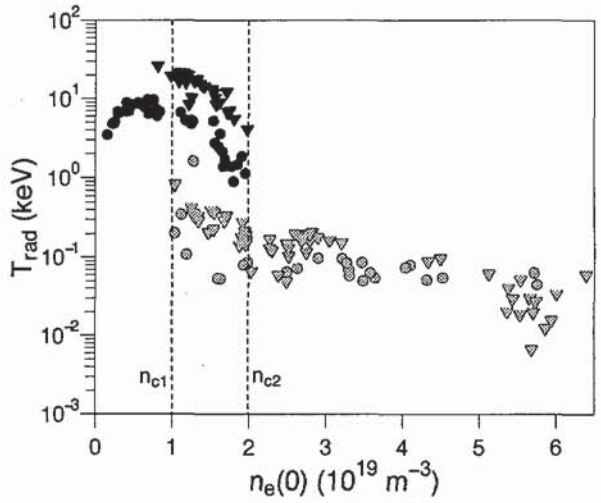

Fig. 4. The LFS (circles) and HFS (triangles) ECE X-mode radiation temperatures at 105.5 GHz indicate the slide-away (black) and the normal ohmic (grey) regimes.

4. HOLLOW TEMPERATURE PROFILES

Steady-state hollow T_e-profiles are reproducibly produced by strong off-axis ECH (110 GHz) in high-density ($n_e(0) > 4.0 \times 10^{19}$ m^{-3}), low current ($I_p \leq 80$ kA) discharges (see Fig. 5a). The steady-state hollow T_e-profile leads to a hollow current density profile and reversed shear in the region inside the resonance

position r_{res}. A new equilibrium is reached typically after 50 ms. Local power balance analysis showed that the net electron heat flux is very small inside r_{res} and may even be directed outwards, i.e. up the gradient of T_e [4]. This points to the existence of an electron heat flux not driven by ∇T, which is confirmed by the propagation of heat pulses induced by modulated ECH [9].

The transition from ohmic to reversed shear profiles has been investigated in more detail. A bifurcation into two levels of confinement appears (see Fig. 5b). The subtlety of the bifurcation is exemplified by one discharge which hesitates and then crosses over from the low to the high confinement branch. The pressure profile for the high confinement branch exhibits a steep gradient near the deposition radius, which is an indication for a region of improved confinement.

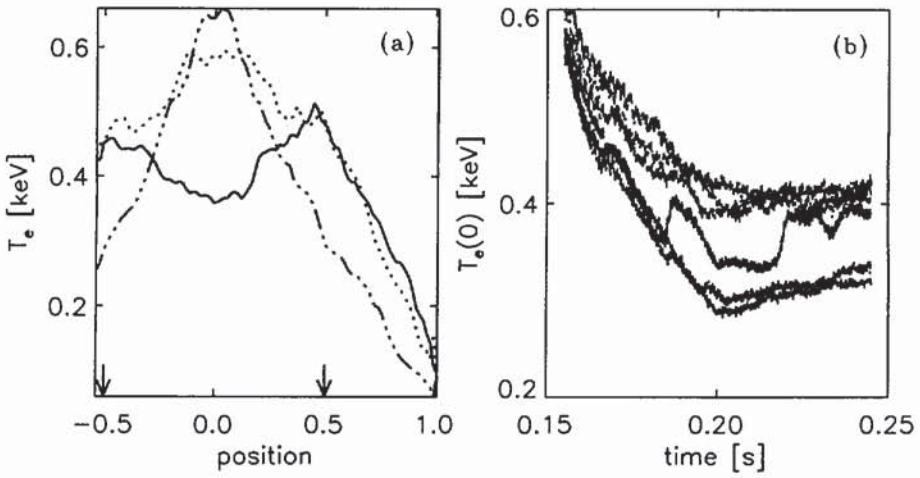

Fig. 5. (a) Evolution of $T_e(r)$ as measured with Thomson scattering in a series of identical discharges. Shown are profiles measured at -1 ms (dotted line), 5 ms (dash-dotted line) and 40 ms (solid line) with respect to the time ECH is switched on. The deposition radius is indicated by arrows. (b) Evolution of $T_e(0)$ as measured by ECE in six near identical discharges after switch on of ECH at t = 150 ms, showing the bifurcation in the confinement.

In all other parts of the plasma the gradients in the pressure profiles for the two branches are rather similar.

In many discharges in the high confinement branch vigorous MHD activity occurs. A fast sawtooth-like relaxation of T_e occurs in a small region around the heat deposition region (rise phase 1 ms, crash phase 200 μs). Moreover, a slower reconnection process takes place throughout the central part of the plasma (rise phase typically 10 ms, crash phase 500 μs). An explanation is sought in terms of double tearing modes. The q-profile derived from $T_e(r)$ after 50 ms, when a new equilibrium is reached, shows a pronounced minimum near the ECH deposition radius with q just below 3. The central value of q is just above 4. The fast modulations are attributed to a double-tearing mode involving the two q=3 surfaces near the deposition radius, whereas the slower process is interpreted as a reconnection process involving both q= 3 surfaces and the central q=4 surface.

5. SAWTOOTH ANALYSIS

Measurements on sawtoothing RTP plasmas with the five-camera 80-channel soft x-ray tomography system were interpreted with a new analysis method that makes use of special functions of the emissivity that are conserved under ideal MHD action [7]. The aim of the study was to find out whether sawteeth in RTP follow the ideal MHD behaviour or whether they show features of reconnection. In particular the influence of the plasma resistivity on the development of the sawtooth instability was investigated. For this purpose a series of discharges in which the magnetic Reynolds number, S, was systematically varied between $(0.8 - 3.5)\times10^5$ has been analysed. With increasing values of S, the m = 1 precursor instability of the sawtooth crash changes from a clear magnetic reconnection behaviour towards a combination of ideal and resistive MHD behaviour. The transition does not seem to be influenced by the absolute pressure value.

6. DISRUPTIONS

A systematic study of the evolution of the T_e, n_e and j-profiles during the thermal and current quench phases of disruptions has been started. The preliminary results seem to confirm earlier observations reported by the DIII-D team [8], that the j-profile only changes at the end of the energy quench. The disruptions were initiated by a rather fast current rise followed by a density ramp-up. Under apparently the same external conditions most of the discharges show strong MHD activity and disrupt at a low density, while in the other discharges the density can be ramped up almost twice as high without major MHD activity. Subtle differences in current penetration must be the cause of this branching. In Fig. 6a

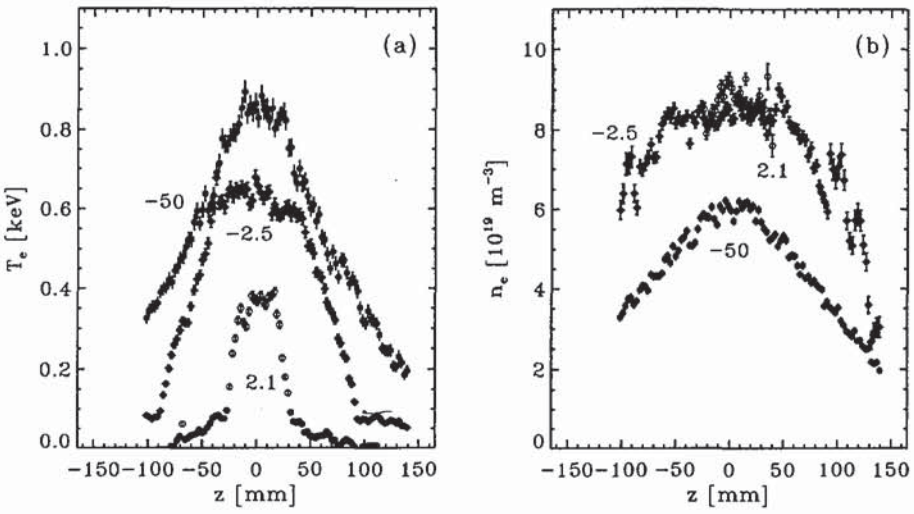

Fig. 6. (a) T_e -profiles 50 and 2.5 ms before the quench of a major disruption of an Ohmic $q_a = 4.2$ discharge and one taken 2.1 ms after the quench during an inward movement of the plasma. (b) The corresponding n_e-profiles.

profiles of T_e are shown at -50, -2.5 and +2.1ms (the start of the current quench is at t =0). The huge m=2 island enforces a cold area between $0.6 < r/a < 1.0$, whilst simultaneously an m=1 structure flattens the T_e-profile for $r/a < 0.3$. Figure 6b shows the corresponding n_e profiles. Due to a vigorous inward movement with 7.5 cm the radius of the plasma column is reduced to 10 cm and the (vertical) Thomson scattering observation chord traverses only the outer part. It should be noticed that the electrons in the centre still have a temperature of at least 400 eV in contrast to ECE measurements which indicate a complete collapse.

ACKNOWLEDGEMENTS

This work was performed under the Euratom-FOM Association agreement with financial support from NWO and Euratom.

REFERENCES

[1] GELDER, J.F.M. van, et al., in Electron Cyclotron Emission and Electron Cyclotron Heating (Proc. 9th Joint Workshop Borrego Spring, 1995), World Scientific, Singapore (1995) 239.
[2] ROMMERS, J.H., HOWARD, J., Plasma Phys. Control. Fusion (in press).
[3] WESTERHOF, E., et al., in Controlled Fusion and Plasma Physics (Proc. 22nd Eur. Conf. Bournemouth, 1995), Vol. 19C, Part I, European Physical Society, Geneva (1995) 385.
[4] HOGEWEIJ, G.M.D., et al., Phys. Rev. Lett. **76** (1996) 632.
[5] SCHOKKER, B.C., PhD thesis, Eindhoven Technical University (1996).
[6] De BAAR, M.R., in Controlled Fusion and Plasma Physics (Proc. 23rd Eur. Conf. Kiev, 1996), Vol. 20C, European Physical Society, Geneva (1996).
[7] TANZI, C.P., et al., Rev. Sci. Instrum. **66** (1995) 537.
[8] TAYLOR, P.L., et al., in Controlled Fusion and Plasma Physics (Proc. 22nd Eur. Conf. Bournemouth, 1995), Vol. 19C, Part IV, European Physical Society, Geneva (1995) 49.
[9] HOGEWEIJ, G.M.D., et al., IAEA-CN-64/AP1-9, these Proceedings, Vol. 1, p. 655.